

Fourier series expansion method for plated-structures

Jiann-Gang Deng† and Fu-Ping Cheng‡

*Department of Civil Engineering, Chiao Tung University,
1001 Ta Hsueh Road, Hsinchu, Taiwan, R.O.C.*

Abstract. This work applies a structural analysis method based on an analytical solution from the Fourier series which transforms a half-range cosine expansion into a static solution involving plated structures. Two sub-matrices of in-plane and plate-bending problems are also formulated and coupled with the prescribed boundary conditions for these variables, thereby providing a convenient basis for a numerical solution. In addition, the plate connection are introduced by describing the connection between common boundary continuity and equilibrium. Moreover, a simple computation scheme is proposed. Numerical results are then compared with finite element results, demonstrating the numerical scheme's versatility and accuracy.

Key words: Fourier series; half-range cosine expansion; in-plane stress; plate-bending stress; plated structures.

1. Introduction

Many civil engineering structures can be classified as fold plate structure systems. Examples include floor, roofs, bridge decks, rectangular storage tanks, and culverts. In regular geometry with simple boundary conditions, a simplified design chart or equations can be used (Moody 1960). However, this solution is not available for complicated geometry and boundary conditions. In recent decades, a finite element method has been used to comprehensively analyze these complicated problems (Irons 1976, Boswell and Zhang 1983, Hrabok and Hrudley 1983). However, this method is seldom employed to analyze plated structures, partially owing to the fact that accurate results depend on the use of a large number of elements. Such a large number of elements require the preparation of a substantial amount of data with large simultaneous equations. Many approximate methods based on physical considerations have been developed (Cheung 1976, Kristek 1979, Puckett and Gutkowski 1986). These techniques were simplified from the finite element method. These methods perform well under certain circumstances. Some boundary element methods have also been proposed to analyze plated structures (Ohga *et al.* 1991), thereby, reducing the size of matrices and input preparation, but a large computation effort in the final integration is still required. However, a more simple, straightforward method has been developed on the basis of an analytical solution. That method also uses the Fourier series expansion

† Ph.D Graduate Student

‡ Associate Professor

transform to boundary conditions. The fact that the solution is based on in-plane stress and on a plate-bending theory, i.e., which is within the scope of the assumptions of superposition, accounts for why the Fourier series expansion method represents an exact method. The solution considers the structure in its actual form as an assemblage of plate-shaped parts which cumulatively forms a real spatial system. The solution does not make any distinction between open and closed cross-sections or multi-celled structures. And various physical properties of the structure's individual parts are also easily introduced into the analysis. Consequently, the proposed method has become a rapid and versatile method for resolving a wide-range of problems involving plated structures.

Two Fourier series expansion methods have been utilized in stress analysis. A numerical procedure for the in-plane stress and plate-bending problems has been proposed (Kang 1993, Deng and Cheng 1997). Solving these governing equations of in-plane stress and plate-bending problems is not a difficult task if the geometry and boundary conditions are not complicated. However, a practical problem likely has a complicated geometry, and must therefore appeal to the numerical method. The boundary condition of a physical problem is easily presented by the Fast Fourier Transform (FFT). A half-plane problem can be constructed by defining a local coordinate system on each edge.

This study applies the analytical solution based on the Fourier series as the solution function of each half-plane problem. By using the solution function, the influence coefficients that relate the Fourier series coefficients of all boundaries to each other can be then analytically derived. In addition, the superposition method is utilized to summarize the influences from all the edges of the domain and, thus, construct a system of equations which can be easily solved. Both in-plane stress and plate-bending are included as well, with each edge having four degrees of freedom. These edge forces and moments are as follows:

- 1) Transverse bending moments M ,
- 2) Shear forces F_V which act perpendicularly to the element plane,
- 3) Longitudinal shear forces F_T ,
- 4) Transverse normal forces F_N acting in the element plane (as Fig. 1).

Their displacements can be described by four components:

- 1) Edge rotation θ ,
- 2) Transverse displacement w normal to the element plane,
- 3) Longitudinal displacement u (along the edge),
- 4) Transverse displacement v in the element plane (normal to the edge).

The positive sense of these rotations and displacements is coincident with the positive sense of the respective edge forces or moments.

Plated structures are formed as an assemblage of plates that are put together, thereby allowing a non-co-planar connection of these plates to satisfy the compatibility and equilibrium conditions.

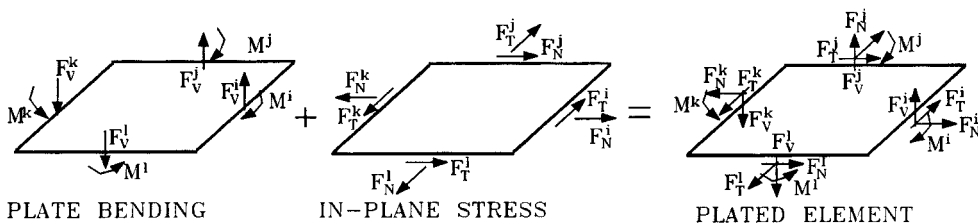


Fig. 1 Combining degree freedoms of plate bending and in plane stress

Herein, we also present an effective scheme to connect plates together, thereby forming plated structures.

2. Fourier series expansion method for in-plane problems

In the following analysis, we use the rectangular Cartesian-coordinate system in which the axes x and y lie in the middle plane of the plate. The governing equations for in-plane problems can be stated as follows, where the gravitational force is absent.

$$\begin{aligned} \frac{\partial \sigma_x}{\partial x} + \frac{\partial \tau_{xy}}{\partial y} - k_d^2 u &= 0 \\ \frac{\partial \tau_{xy}}{\partial x} + \frac{\partial \sigma_y}{\partial y} - k_d^2 v &= 0 \quad \text{in } \Omega \end{aligned} \quad (1a)$$

$$\begin{aligned} u &= d_1(s), \quad v = d_2(s) \quad \text{on } \partial\Omega_1 \\ F_N &= d_3(s), \quad F_T = d_4(s) \quad \text{on } \partial\Omega_2 \end{aligned} \quad (1b)$$

where k_d denotes the equivalent spring constant of the elastic foundation. To numerically treat it, the constant term of an analytical solution, k_d is introduced. For the problem without an elastic foundation, an extremely small k_d is used. E , ν denotes elastic modulus and Poisson's ratio respectively. In addition, Ω represents a polygonal domain (Fig. 2), where $\partial\Omega_1 + \partial\Omega_2 = \partial\Omega$ denotes the boundary of Ω . If nhj series terms are used, the general solution of Eq. (1a) can be obtained as follows:

$$u = \sum_{n=1}^{nhj} a_n \times e^{-p_n y} \sin(\lambda_n x) + b_n \times e^{-q_n y} \sin(\lambda_n x) \quad (2a)$$

$$v = a_0 \times e^{-q_0 x} + b_0 \times e^{-p_0 y} + \sum_{n=1}^{nhj} a_n \times c_n e^{-p_n y} \cos(\lambda_n x) + b_n \times d_n e^{-q_n y} \cos(\lambda_n x) \quad (2b)$$

where $p_0 = k_d$, $q_0 = k_d \times \sqrt{2/(1-\nu)}$, $P_n = \sqrt{\lambda_n^2 + k_d^2}$

$$q_n = \sqrt{\lambda_n^2 + k_d^2 \times 2/(1-\nu)}, \quad c_n = p_n / \lambda_n, \quad d_n = q_n / \lambda_n, \quad \lambda_n = n \pi / l_j$$

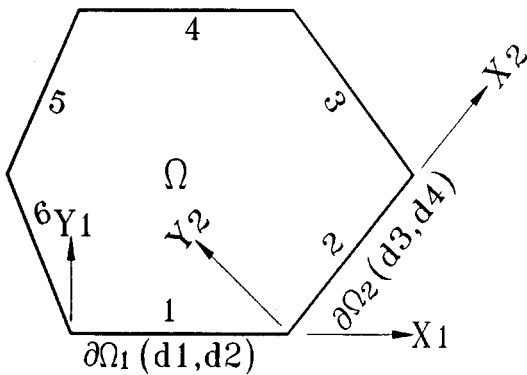


Fig. 2 Edge coordinate system of an analysis plane

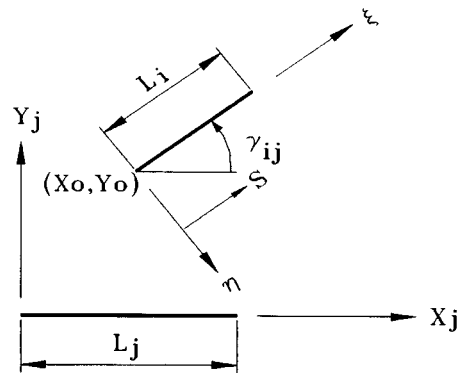


Fig. 3 Coordinate transform on edges i and j

where l_j is the half period of the boundary condition prescribed on the boundary segment j (Fig. 3), λ_n represents mode number of l_j , unknown coefficients a_n , b_n are amplitudes of mode n .

According to Fig. 2, the displacements of each edge of the domain must satisfy the solution for the governing equations. In addition, influence coefficients on any edge can be calculated from its local coordinate and the other edges. As an example of edge i, j (Fig. 3), when displacement u_j, v_j are held on edge j , the influence of the displacements and forces on edge i can be calculated from the coordinate transformation as

$$u_j^i = u_j \times \cos \gamma_{ij} + v_j \times \sin \gamma_{ij} \quad (3a)$$

$$v_j^i = u_j \times \sin \gamma_{ij} - v_j \times \cos \gamma_{ij} \quad (3b)$$

$$(F_N)_j^i = \frac{E}{1-\nu^2} \times \{ (u_j)_x \times (\sin^2 \gamma_{ij} + \nu \times \cos^2 \gamma_{ij}) + (v_j)_y \times (\cos^2 \gamma_{ij} + \nu \times \sin^2 \gamma_{ij}) - (1-\nu) \times ((u_j)_y + (v_j)_x) \times \sin \gamma_{ij} \cos \gamma_{ij} \} \quad (3c)$$

$$(F_T)_j^i = \frac{E}{2(1+\nu)} \times \{ (v_j)_x \times (\sin^2 \gamma_{ij} - \cos^2 \gamma_{ij}) + (u_j)_y \times (\sin^2 \gamma_{ij} - \cos^2 \gamma_{ij}) + ((u_j)_x - (v_j)_y) \times \sin 2\gamma_{ij} \} \quad (3d)$$

where γ_{ij} denotes the angle between lines j and i . $(u_j)_x, (u_j)_y, (v_j)_x, (v_j)_y$ are derivatives of u_j, v_j . These $u_j^i, v_j^i, F_{Nj}^i, F_{Tj}^i$ terms can be expanded by half-range cosine expansion, the m th influence function term of edge i from edge j can be expressed as:

$$(u_m)_j^i = \sum_{n=0}^{nhj-1} ((u_{1mn})_j^i \times a_n^i + (u_{2mn})_j^i \times b_n^i) \quad (4a)$$

$$(v_m)_j^i = \sum_{n=0}^{nhj-1} ((v_{1mn})_j^i \times a_n^i + (v_{2mn})_j^i \times b_n^i) \quad (4b)$$

$$((F_N)_m)_j^i = \sum_{n=0}^{nhj-1} ((s_{1mn})_j^i \times a_n^i + (s_{2mn})_j^i \times b_n^i) \quad (4c)$$

$$((F_T)_m)_j^i = \sum_{n=0}^{nhj-1} ((t_{1mn})_j^i \times a_n^i + (t_{2mn})_j^i \times b_n^i) \quad (4d)$$

Details of how to calculate $(u_{1mn})_j^i, (u_{2mn})_j^i, (v_{1mn})_j^i, (v_{2mn})_j^i, (s_{1mn})_j^i, (s_{2mn})_j^i, (t_{1mn})_j^i, (t_{2mn})_j^i$, can be found elsewhere (Deng and Cheng 1997).

In the domain of a half plane (Fig. 3), for an arbitrary boundary condition $d_j(x)$ on line j , it can be expanded by a half-range cosine expansion along line j . If mhj harmonics have been employed, it can be expressed as

$$d_j(x) = \sum_{m=0}^{mhj-1} (d_m)_j \times \cos(\alpha_m x) \quad (5)$$

where $\alpha_m = m\pi/l_j$, 1_j denotes the length of the line j , and $(d_m)_j$ represents the half-range cosine coefficients of the function of $d_j(x)$. Four possible types of the admissible boundary conditions are defined as follows:

$$bc_1^s = \begin{Bmatrix} u \\ v \end{Bmatrix}, \quad bc_2^s = \begin{Bmatrix} F_N \\ F_T \end{Bmatrix}, \quad bc_3^s = \begin{Bmatrix} v \\ F_T \end{Bmatrix}, \quad bc_4^s = \begin{Bmatrix} F_N \\ u \end{Bmatrix}$$

For each boundary, the coefficients of any series of terms expanded by a half-range cosine expansion must have the same value as the prescribed boundaries. According to Eqs. (4), (5), boundary conditions can be expressed as

$$\begin{bmatrix} (DM_{mn})_1^1 & (DM_{mn})_2^1 & \cdots & (DM_{mn})_M^1 \\ (DM_{mn})_1^2 & (DM_{mn})_2^2 & \cdots & (DM_{mn})_M^2 \\ \vdots & \vdots & (DM_{mn})_j^i & \vdots \\ (DM_{mn})_1^N & (DM_{mn})_2^N & \cdots & (DM_{mn})_M^N \end{bmatrix} \begin{bmatrix} (C_n)^1 \\ (C_n)^2 \\ \vdots \\ (C_n)^N \end{bmatrix} = \begin{bmatrix} (d_m)_1 \\ (d_m)_2 \\ \vdots \\ (d_m)_M \end{bmatrix} \quad (6)$$

For the boundary of $\{bc_1^s\}$, $\{bc_2^s\}$, the influence coefficients matrix and their corresponding boundary conditions can be found as follow:

$$(DM_{mn})_j^i = \begin{bmatrix} (u_{1mn})_j^i & (u_{2mn})_j^i \\ (v_{1mn})_j^i & (v_{2mn})_j^i \end{bmatrix}, \quad \{d_m\}_j = \begin{Bmatrix} (u_m)_j \\ (v_m)_j \end{Bmatrix} \quad (7a)$$

$$(FM_{mn})_j^i = \begin{bmatrix} (s_{1mn})_j^i & (s_{2mn})_j^i \\ (t_{1mn})_j^i & (t_{2mn})_j^i \end{bmatrix}, \quad \{f_m\}_j = \begin{Bmatrix} ((F_N)_m)_j \\ ((F_T)_m)_j \end{Bmatrix} \quad (7b)$$

For brevity sake, Eq. (7) can be replaced as

$$[DM] \times \{C\} = \{d\}, \quad [FM] \times \{C\} = \{f\} \quad (8)$$

By eliminating the unknown term $\{C\}$ of Eq. (8), the relation between displacements and forces along the boundary can be expressed in a matrix form as

$$\begin{bmatrix} K_N \\ K_T \end{bmatrix} \times \begin{Bmatrix} u \\ v \end{Bmatrix} = \begin{Bmatrix} F_N \\ F_T \end{Bmatrix} \quad (9)$$

3. Fourier series expansion method for plate-bending problems

The governing equation of the plate-bending problem is a bi-harmonic equation. For a homogeneous, isotropic, elastic plate on an elastic foundation, the equation is

$$\nabla^4 w + k_s^4 w = q/D \quad \text{in } \Omega \quad (10a)$$

$$\begin{aligned} w &= d_1(s), \quad \chi_\eta = d_2(s) \quad \text{on } \partial\Omega_1 \\ M_\eta &= d_3(s), \quad (F_V)_\eta = d_4(s) \quad \text{on } \partial\Omega_2 \end{aligned} \quad (10b)$$

where D is the flexural rigidity of the plate, and q is the load applied to the plate. The reason for introducing k_s has been mentioned earlier. Solutions of Eq. (10a) include both the complementary solution and the particular solution as

$$w(x, y) = w^c(x, y) + w^p(x, y) \quad (11)$$

where, superscripts c and p represent the complementary solution and the particular solution respectively.

3.1. Complementary solution

The homogeneous part of Eq. (10a) is described as:

$$\nabla^4 w^c + k_d^4 w^c = 0 \quad (12)$$

Herein, we select the exponentially decaying part of general solution of Eq. (12) as the solution function (Timoshenko and Woinowsky-Krieger 1959). If nhj series are used, the complementary solution is the summation of all the series as

$$w^c(x, y) = \sum_{n=0}^{nhj-1} (A_n \cos \beta_n y + B_n \sin \beta_n y) e^{-\mu_n y} \cos \lambda_n x \quad (13)$$

where $\lambda_n = n\pi/l_j$, $\mu_n = \sqrt{(\sqrt{\lambda_n^4 + k_d^4} + \lambda_n^2)/2}$, $\beta_n = \sqrt{(\sqrt{\lambda_n^4 + k_d^4} - \lambda_n^2)/2}$, A_n , B_n are amplitude of n th harmonic.

Again, we attempt to construct the influence coefficient matrix of each edge. As an example of edge i , j , when displacement w^c are held on edge j , the influence of rotation, bending moment, twist moment, effective shear on edge i can be calculated from the coordinate transformation as

$$\chi_\eta = -\frac{\partial w^c}{\partial x} \sin \gamma_{ij} + \frac{\partial w^c}{\partial y} \cos \gamma_{ij} \quad (14a)$$

$$M_\eta = \frac{1}{2}(M_x + M_y) - \frac{1}{2}(M_x - M_y) \cos 2\gamma_{ij} - M_{xy} \sin 2\gamma_{ij} \quad (14b)$$

$$M_{\eta\xi} = \frac{1}{2}(M_x - M_y) \sin 2\gamma_{ij} - M_{xy} \cos 2\gamma_{ij} \quad (14c)$$

$$(F_V)_\eta = -D \frac{\partial(\Delta w^c)}{\partial \eta} + \frac{\partial M_{\eta\xi}}{\partial \xi} \quad (14d)$$

Definitions of M_x , M_y , M_{xy} , Δw^c can be found elsewhere (Timoshenko and Woinowsky-Krieger 1959). These w^c , χ_η , M_η , $(F_V)_\eta$ terms can be expanded by half-range cosine expansion, the m th influence function term of edge i from edge j , can be expressed as:

$$(w_m^c)^j = \sum_{j=1}^N \sum_{n=0}^{nhj-1} ((W1_{mn})_j^i A_n^j + (W2_{mn})_j^i B_n^j) \quad (15a)$$

$$((\chi_\eta)_m)^j = \sum_{j=1}^N \sum_{n=0}^{nhj-1} ((S1_{mn})_j^i A_n^j + (S2_{mn})_j^i B_n^j) \quad (15b)$$

$$((M_\eta)_m)^i = \sum_{j=1}^N \sum_{n=0}^{nhj-1} ((M1_{mn})_j^i A_n^j + (M2_{mn})_j^i B_n^j) \quad (15c)$$

$$((F_{V\eta})_m)^i = \sum_{j=1}^N \sum_{n=0}^{nhj-1} ((V1_{mn})_j^i A_n^j + (V2_{mn})_j^i B_n^j) \quad (15d)$$

Details of how to calculate $(W1_{mn})_j^i$, $(W2_{mn})_j^i$, $(S1_{mn})_j^i$, $(S2_{mn})_j^i$, $(M1_{mn})_j^i$, $(M2_{mn})_j^i$, $(V1_{mn})_j^i$, $(V2_{mn})_j^i$ can be found in Kang (1993).

Four possible admissible boundary conditions are defined as follows:

$$\{bc_1^p\} = \begin{Bmatrix} \chi_\eta \\ w \end{Bmatrix}, \{bc_2^p\} = \begin{Bmatrix} M_\eta \\ F_{V\eta} \end{Bmatrix}, \{bc_3^p\} = \begin{Bmatrix} M_\eta \\ w \end{Bmatrix}, \{bc_4^p\} = \begin{Bmatrix} \chi_\eta \\ F_{V\eta} \end{Bmatrix} \quad (16)$$

Following the same procedure as we described above, the coefficients of any series term can be expanded by a half-range cosine expansion to form the influence coefficient matrix and the boundary vectors. For the boundary of $\{bc_1^p\}$ and $\{bc_2^p\}$, the influence coefficients matrix and corresponding boundary conditions can be found as follows:

$$(DM_{mn})_j^i = \begin{bmatrix} [S1_{mn}]_j^i & [S2_{mn}]_j^i \\ [W1_{mn}]_j^i & [W2_{mn}]_j^i \end{bmatrix}, \quad \{d_m\}_j = \begin{Bmatrix} \{(\chi_\eta)_m\}_j \\ \{w_m^c\}_j \end{Bmatrix} \quad (17a)$$

$$(FM_{mn})_j^i = \begin{bmatrix} [M1_{mn}]_j^i & [M2_{mn}]_j^i \\ [V1_{mn}]_j^i & [V2_{mn}]_j^i \end{bmatrix}, \quad \{f_m\}_j = \begin{Bmatrix} \{(M_\eta)_m\}_j \\ \{(F_{V\eta})_m\}_j \end{Bmatrix} \quad (17b)$$

The relation between the displacements and forces can be expressed in a matrix form

$$\begin{bmatrix} Km \\ Kv \end{bmatrix} \times \begin{Bmatrix} \chi_\eta \\ w \end{Bmatrix} = \begin{Bmatrix} M_\eta \\ F_{V\eta} \end{Bmatrix} \quad (18)$$

3.2. Particular solution

Consider a non-homogeneous governing Eq. (10a), i.e.,

$$\nabla^4 w^p + k_d^4 w^p = q(x, y) \quad (19)$$

For any function $q(x, y)$ over the rectangular domain, its corresponding Fourier coefficients can be calculated by the following equation:

$$q(x, y) = \sum_{l=0}^{\infty} Q_{ln} \cos \lambda_l x \cos \beta_n y \quad (20)$$

where $\lambda_l = l\pi/a$, $\beta_n = n\pi/b$, a , b are dimensions of the encompassed rectangular (Fig. 2). A two

dimensional Fast Fourier Transform is used for calculating the Fourier coefficients Q_{ln} .

The solution of Eq. (19) is assumed to be

$$w^p = W_{00}^p \left(x - \frac{a}{2} \right)^4 + \sum_{l=0}^{\infty} \sum_{n=0}^{\infty} W_{ln}^p \cos \lambda_l x \cos \beta_n y \quad (21)$$

The Fourier coefficients of the contributions of the polynomial part, Eq. (21), are

$$(w_m^p)_p(s) = W_{00}^p (X4)_m \quad (22a)$$

$$((\chi_\eta^p)_m)_p(s) = -4 \sin \phi_i W_{00}^p (X3)_m \quad (22b)$$

$$((M_\eta^p)_m)_p(s) = -6D [(1+\nu) - (1-\nu) \cos 2\phi_i] W_{00}^p (X2)_m \quad (22c)$$

$$((F_{V\eta}^p)_m)_p(s) = -24D [1+(1-\nu) \cos 2\phi_i] \sin \phi_i W_{00}^p (X1)_m \quad (22d)$$

The Fourier coefficients of the contributions of the series part Eq. (21), are

$$(W_m^p)_s = \sum_{l=0}^{nhj-1} \sum_{n=0}^{nhj-1} W_{ln}^p CC_{lnm} \quad (23a)$$

$$((\chi_\eta^p)_m)_s = \sum_{l=0}^{nhj-1} \sum_{n=0}^{nhj-1} W_{ln}^p [\lambda SC_{lnm} \sin \phi_i - \beta_n CS_{lnm} \cos \phi_i] \quad (23b)$$

$$((M_\eta^p)_m)_s = \sum_{l=0}^{nhj-1} \sum_{n=0}^{nhj-1} W_{ln}^p [MS_{lnm} - MD_{lnm} \cos 2\phi_i - MT_{lnm} \sin 2\phi_i] \quad (23c)$$

$$((F_{V\eta}^p)_m)_s = \sum_{l=0}^{nhj-1} \sum_{n=0}^{nhj-1} W_{ln}^p [VS_{lnm} \sin \phi_i - VC_{lnm} \cos \phi_i] \quad (23d)$$

subscript p , s , refers to the polynomial and series parts respectively. How to calculate $(X4)_m$, $(X3)_m$, $(X2)_m$, $(X1)_m$ and $(MS)_{lnm}$, $(MD)_{lnm}$, $(MT)_{lnm}$, $(VC)_{lnm}$, $(VS)_{lnm}$ can be found in Kang (1993).

Summing up the contributions from both the polynomial part and series parts, the particular boundary condition is obtained as

$$\{d_m^p\}_j = \left\{ \begin{array}{l} ((\chi_\eta^p)_m)_{p,j} + ((\chi_\eta^p)_m)_{s,j} \\ (w_m^p)_{p,j} + (w_m^p)_{s,j} \end{array} \right\}, \quad \{f_m^p\}_j = \left\{ \begin{array}{l} ((M_\eta^p)_m)_{p,j} + ((M_\eta^p)_m)_{s,j} \\ ((F_{V\eta}^p)_m)_{p,j} + ((F_{V\eta}^p)_m)_{s,j} \end{array} \right\} \quad (24)$$

The total solution is the sum of the complementary solution and the particular solution

$$\{d^t\} = \{d^c\} + \{d^p\} \quad (25)$$

substituting $\{d^c\}$ of Eq. (25) to Eq. (18). Relations of displacements and forces can be established as

$$\begin{bmatrix} Km \\ Kv \end{bmatrix} \times \begin{Bmatrix} \chi_\eta^t \\ w^t \end{Bmatrix} = \begin{bmatrix} Km \\ Kv \end{bmatrix} \times \begin{Bmatrix} \chi_\eta^p \\ w^p \end{Bmatrix} + \left(\begin{Bmatrix} M_\eta^t \\ F_{V\eta}^t \end{Bmatrix} - \begin{Bmatrix} M_\eta^p \\ F_{V\eta}^p \end{Bmatrix} \right) \quad (26)$$

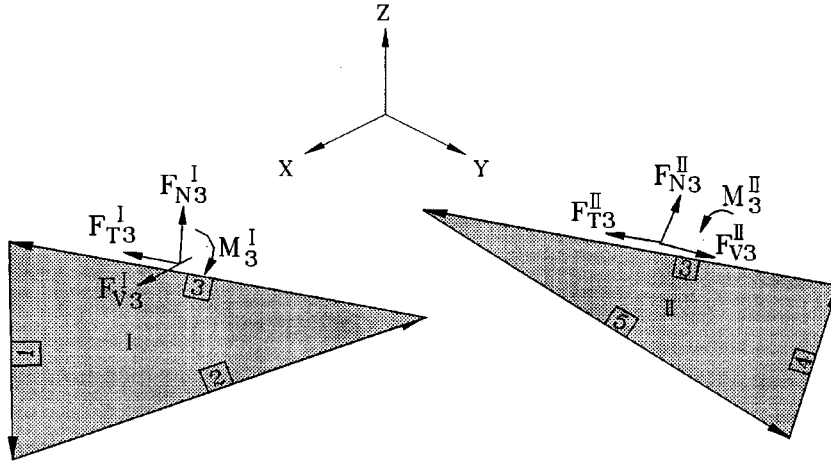


Fig. 4 Equilibrium of connection boundary

4. Connection of plates

The two plates can be connected by understanding the relationship between equilibrium and compatibility of the common boundary. As Fig. 4 indicates, non co-planar plates I and II have the common boundary line 3. The fact that the vector of Fourier coefficients defined on any boundary are directional accounts shows why the negative direction on line 3 between plates I and II, has a negative value from the cosine expansion in odd terms. The Fourier coefficient vectors that belong to the common boundary are then transferred to the same direction defined herein. Next a transformation of vector $\{A\}$ is introduced as

$$\{\hat{A}_m\} = (-1)^{m+1} \times \{A_m\} \quad (27)$$

From the common boundary compatibility, the relation between displacements u , v , w and rotation χ of plates I, II can be described as

$$\{\chi_3\}^{II} = -\{\hat{\chi}_3\}^I \quad (28a)$$

$$\{w_3\}^{II} = \{\hat{w}_3\}^I \times \cos \theta + \{\hat{u}_3\}^I \times \sin \theta \quad (28b)$$

$$\{u_3\}^{II} = \{\hat{w}_3\}^I \times \sin \theta - \{\hat{u}_3\}^I \times \cos \theta \quad (28c)$$

$$\{v_3\}^{II} = -\{\hat{v}_3\}^I \quad (28d)$$

as $\{d_s\}$, $\{d_p\}$ stands in-plane as plate-bending displacements vector substitute $\{d_s\}$, $\{d_p\}$ to Eq. (25)

$$\{d_{p3}^t\}^{II} = \{\hat{d}_{p3}^t\}^I \times [t_{pp}] + \{\hat{d}_{s3}\}^I \times [t_{ps}] \quad (29a)$$

$$\{d_{s3}\}^{II} = \{\hat{d}_{p3}^t\}^I \times [t_{sp}] + \{\hat{d}_{s3}\}^I \times [t_{ss}] \quad (29b)$$

where $[t_{pp}] = \begin{bmatrix} 1 & 0 \\ 0 & \cos \theta \end{bmatrix}$, $[t_{ps}] = \begin{bmatrix} 0 & 0 \\ 0 & \sin \theta \end{bmatrix}$, $[t_{sp}] = [t_{ps}]$, $[t_{ss}] = -[t_{pp}]$.

According to the common boundary's equilibrium, the relation between forces F_v , F_N , F_T along with bending moment M of plates I, II can be described as

$$\{M_3^I\}^I = \{\hat{M}_3^I\}^{II} \quad (30a)$$

$$\{F_{V3}^I\}^I = -\{\hat{F}_{v3}^I\}^{II} \times \cos \theta - \{\hat{F}_{N3}^I\}^{II} \times \sin \theta \quad (30b)$$

$$\{F_{N3}^I\}^I = -\{\hat{F}_{v3}^I\}^{II} \times \sin \theta + \{\hat{F}_{N3}^I\}^{II} \times \cos \theta \quad (30c)$$

$$\{F_{T3}^I\}^I = \{\hat{F}_{T3}^I\}^{II} \quad (30d)$$

By combining Eq. (18) and Eq. (30) the force along common boundary 3 of plate I can be expressed as

$$\{M_3^I\}^I = [Km_{31}]^I \{d_{p1}^c\}^I + [Km_{32}]^I \{d_{p2}^c\}^I + [Km_{33}]^I \{d_{p3}^c\}^I + \{M_3^p\}^I \quad (31a)$$

$$\{F_{V3}^I\}^I = [Kv_{31}]^I \{d_{p1}^c\}^I + [Kv_{32}]^I \{d_{p2}^c\}^I + [Kv_{33}]^I \{d_{p3}^c\}^I + \{F_{V3}^p\}^I \quad (31b)$$

$$\{F_{N3}^I\}^I = [Kn_{31}]^I \{d_{s1}^c\}^I + [Kn_{32}]^I \{d_{s2}^c\}^I + [Kn_{33}]^I \{d_{s3}^c\}^I \quad (31c)$$

$$\{F_{T3}^I\}^I = [Kt_{31}]^I \{d_{s1}^c\}^I + [Kt_{32}]^I \{d_{s2}^c\}^I + [Kt_{33}]^I \{d_{s3}^c\}^I \quad (31d)$$

the force along common boundary 3 of plate II can be expressed as

$$\{M_3^I\}^{II} = [Km_{33}]^{II} \{d_{p3}^c\}^{II} + [Km_{34}]^{II} \{d_{p4}^c\}^{II} + [Km_{35}]^{II} \{d_{p5}^c\}^{II} + \{M_3^p\}^{II} \quad (32a)$$

$$\{F_{V3}^I\}^{II} = [Kv_{33}]^{II} \{d_{p3}^c\}^{II} + [Kv_{34}]^{II} \{d_{p4}^c\}^{II} + [Kv_{35}]^{II} \{d_{p5}^c\}^{II} + \{F_{V3}^p\}^{II} \quad (32b)$$

$$\{F_{N3}^I\}^{II} = [Kn_{33}]^{II} \{d_{s3}^c\}^{II} + [Kn_{34}]^{II} \{d_{s4}^c\}^{II} + [Kn_{35}]^{II} \{d_{s5}^c\}^{II} \quad (32c)$$

$$\{F_{T3}^I\}^{II} = [Kt_{33}]^{II} \{d_{s3}^c\}^{II} + [Kt_{34}]^{II} \{d_{s4}^c\}^{II} + [Kt_{35}]^{II} \{d_{s5}^c\}^{II} \quad (32d)$$

By substituting Eqs. (31), (32) into Eq. (30), the unknown displacement Fourier coefficient vectors of the common boundary can be written as

$$\begin{bmatrix} K_{mp} & K_{ms} \\ K_{vp} & K_{vs} \\ K_{np} & K_{ns} \\ K_{tp} & K_{ts} \end{bmatrix} \times \begin{bmatrix} \{d_{p3}^I\}^I \\ \{d_{s3}^I\}^I \end{bmatrix} = \begin{Bmatrix} R_M \\ R_V \\ R_N \\ R_T \end{Bmatrix} \quad (33)$$

where

$$[K_{mp}] = [Km_{33}]^I - [\widetilde{\widetilde{K}} m_{33}]^{II} \times [t_{pp}], \quad [K_{ms}] = -[\widetilde{\widetilde{K}} m_{33}]^{II} \times [t_{ps}]$$

$$[K_{vp}] = [Kv_{33}]^I + [\widetilde{\widetilde{K}} v_{33}]^{II} \times [t_{pp}] \times \cos \theta + [\widetilde{\widetilde{K}} n_{33}]^{II} \times [t_{ps}] \times \sin \theta$$

$$[K_{vs}] = [\widetilde{\widetilde{K}} v_{33}]^{II} \times [t_{ps}] \times \cos \theta + [\widetilde{\widetilde{K}} n_{33}]^{II} \times [t_{ss}] \times \sin \theta$$

$$[K_{np}] = [\widetilde{\widetilde{K}} v_{33}]^{II} \times [t_{pp}] \times \sin \theta - [\widetilde{\widetilde{K}} n_{33}]^{II} \times [t_{sp}] \times \cos \theta$$

$$\begin{aligned}
[K_{ns}] &= [Kn_{33}]^I + \left[\widetilde{\bar{K}} v_{33} \right]^{II} \times [t_{ps}] \times \sin \theta - \left[\widetilde{\bar{K}} n_{33} \right]^{II} \times [t_{sp}] \times \cos \theta \\
[K_{lp}] &= \left[\widetilde{\bar{K}} t_{33} \right]^{II} \times [t_{sp}], [K_{ts}] = [Kt_{33}]^{II} - \left[\widetilde{\bar{K}} t_{33} \right]^{II} \times [t_{ss}] \\
\{R_M\} &= -[Km_{31}]^I \times (\{d'_{p1}\}^I - \{d^p_{p1}\}^I) - [Km_{32}]^I \times (\{d'_{p2}\}^I - \{d^p_{p2}\}^I) + [Km_{33}]^I \times \{d^p_{p3}\}^I \\
&\quad - \left[\widetilde{\bar{K}} m_{33} \right]^{II} [t_{pp}] \{d^p_{p3}\}^I + \left[\bar{K} m_{34} \right]^{II} (\{d'_{p4}\}^{II} - \{d^p_{p4}\}^{II}) + \left[\bar{K} m_{35} \right]^{II} (\{d'_{p5}\}^{II} - \{d^p_{p5}\}^{II}) \\
&\quad - \{M_3^p\}^I + \{\bar{M}_3^p\}^{II} \\
\{R_V\} &= -[Kv_{31}]^I \times (\{d'_{p1}\}^I - \{d^p_{p1}\}^I) - [Kv_{32}]^I \times (\{d'_{p2}\}^I - \{d^p_{p2}\}^I) + [Kv_{33}]^I \times \{d^p_{p3}\}^I \\
&\quad + \left(\left[\widetilde{\bar{K}} v_{33} \right]^{II} [t_{pp}] \{d^p_{p3}\}^I - \left[\bar{K} v_{34} \right]^{II} (\{d'_{p4}\}^{II} - \{d^p_{p4}\}^{II}) - \left[\bar{K} v_{35} \right]^{II} (\{d'_{p5}\}^{II} - \{d^p_{p5}\}^{II}) \right) \\
&\quad \times \cos \theta - \left(\left[\bar{K} n_{34} \right]^{II} \{d_{s4}\}^{II} + \left[\bar{K} n_{35} \right]^{II} \{d_{s5}\}^{II} \right) \times \sin \theta - \{F_{v3}^p\}^I + \{\bar{F}_{v3}^p\}^{II} \times \cos \theta \\
\{R_N\} &= -[Kn_{31}]^I \{d_{s1}\}^I - [Kn_{32}]^I \{d_{s2}\}^I \\
&\quad + \left(\left[\widetilde{\bar{K}} v_{33} \right]^{II} [t_{pp}] \{d^p_{p3}\}^I + \left[\bar{K} v_{34} \right]^{II} (\{d'_{p4}\}^{II} - \{d^p_{p4}\}^{II}) + \left[\bar{K} v_{35} \right]^{II} (\{d'_{p5}\}^{II} - \{d^p_{p5}\}^{II}) \right) \\
&\quad \times \sin \theta - \left(\left[\bar{K} n_{33} \right]^{II} [t_{sp}] \{d^p_{p3}\}^I - \left[\bar{K} n_{34} \right]^{II} \{d_{s4}\}^{II} - \left[\bar{K} n_{35} \right]^{II} \{d_{s5}\}^{II} \right) \times \cos \theta \\
&\quad + \left\{ \bar{F}_{v3}^p \right\}^{II} \times \sin \theta
\end{aligned}$$

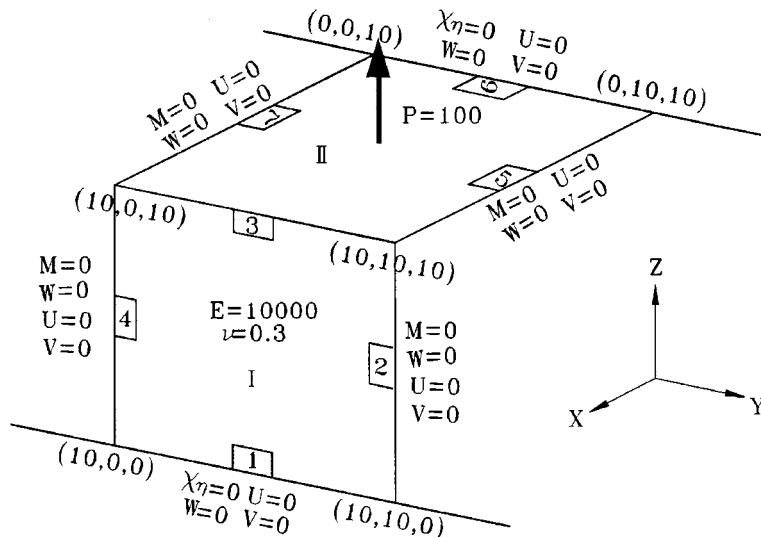


Fig. 5 Example of two orthogonal plane under a surface uniform load

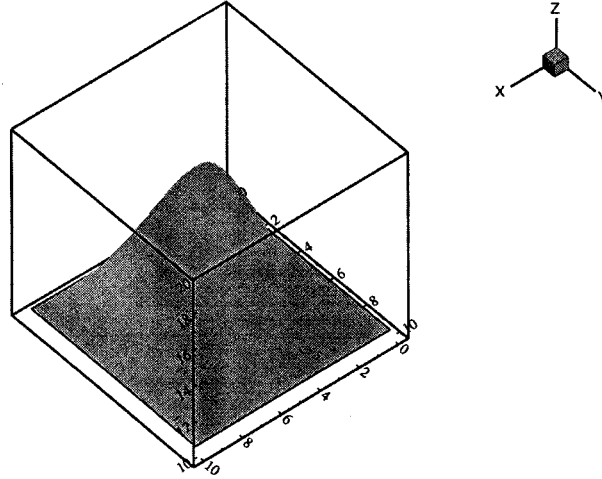
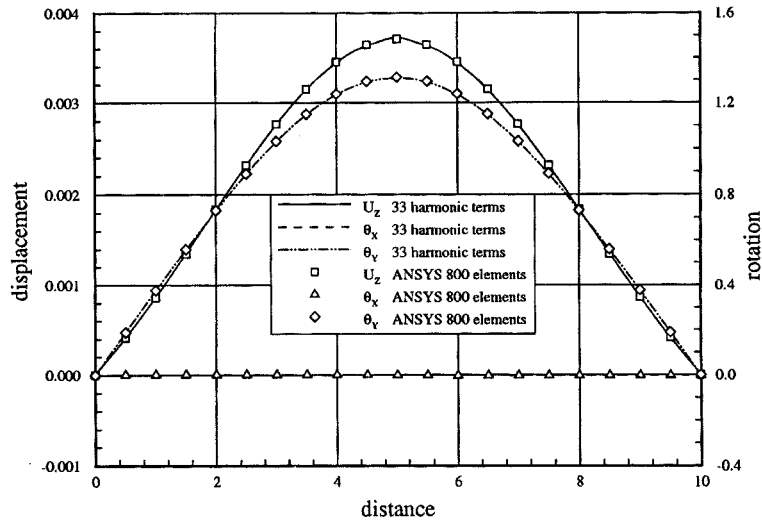


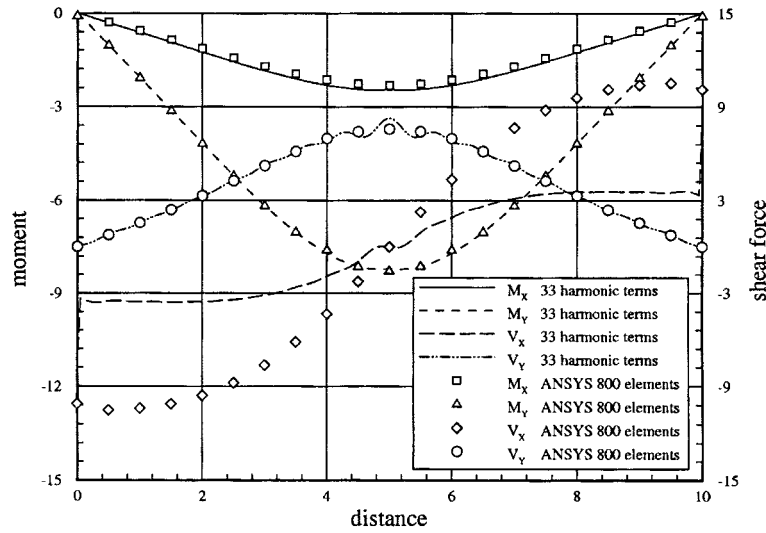
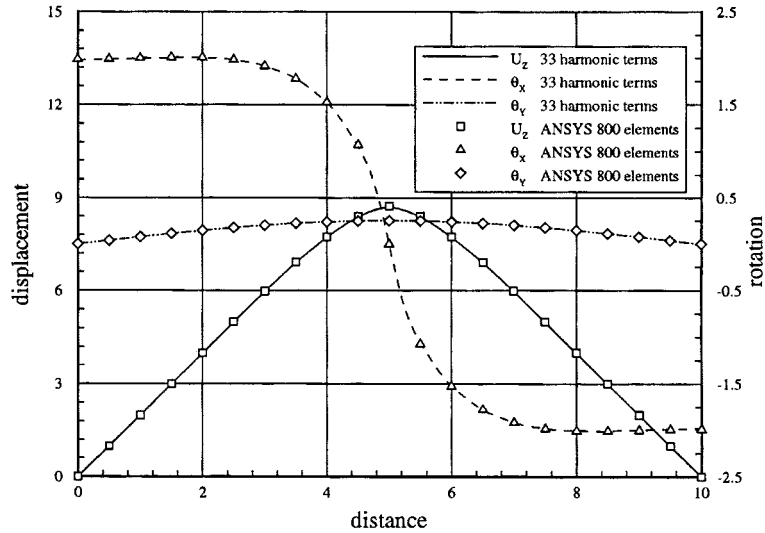
Fig. 6 Surface deformed shape of plate II

Fig. 7 Comparison of displacement and rotation along $x=10$, plate II

$$\begin{aligned} \{R_T\} = & -[Kt_{31}]^I \{d_{s1}\}^I - [Kt_{32}]^I \{d_{s2}\}^I - [\widetilde{K} t_{33}]^{II} [t_{sp}] \{d_{p3}^p\}^I + [\overline{K} t_{34}]^{II} \{d_{s4}\}^{II} \\ & + [\overline{K} t_{35}]^{II} \{d_{s5}\}^{II} \end{aligned}$$

where $[\overline{K}]$ and $[\widetilde{K}]$ denote the row and column transformation of $[K]$ respectively.

Eq. (33) has constructed a system of simultaneous equations. It can be easily solved by any linear equation solver to obtain $\{d_{p3}^p\}^I$, $\{d_{s3}\}^I$. Furthermore, $\{d_{p3}^p\}^{II}$ and $\{d_{s3}\}^{II}$ can be obtained by substituting $\{d_{p3}^p\}^I$ and $\{d_{s3}\}^I$ into Eq. (28) as well. Unknown coefficients of amplitude $\{a_n\}$, $\{b_n\}$, $\{A_n\}$, and $\{B_n\}$, of each edge can be easily solved from Eq. (6), respectively. Therefore, displacements u , v , w , χ and forces M , F_v , F_b , F_T on any point of the domain can be easily calculated.

Fig. 8 Comparison of moment and shear force along $x=10$, plate IIFig. 9 Comparison of displacement and rotation along $x=5$, plate II

5. Numerical example

The proposed method's accuracy is demonstrated by examining a problem which involves two orthogonal plates with a simple geometry under a concentrated load (as illustrated in Fig. 5). For a rectangular plate having a size of 10×10 and a thickness of 0.1 unit, the complicated boundary involving simple and fixed supports is assumed. The boundary conditions of both in-plane stress and plate-bending of plate I are

$$\{d_s\}^I = \{bc_1^s \ bc_1^s \ bc_1^s \ bc_1^s\}^I, \quad \{d_p\}^I = [bc_1^p \ bc_3^p \ bc_1^p \ bc_3^p]^I$$

and plate II are

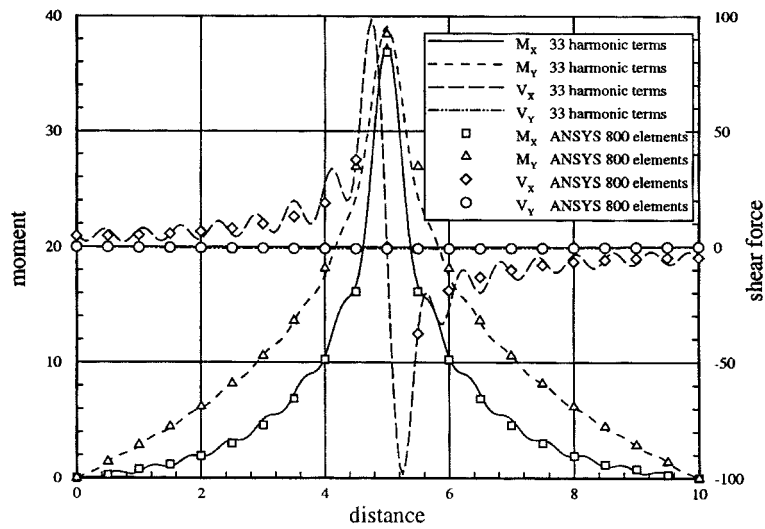
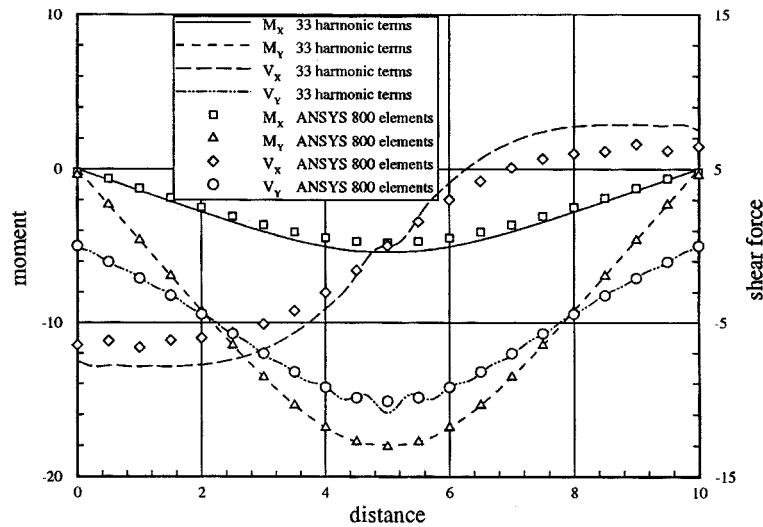
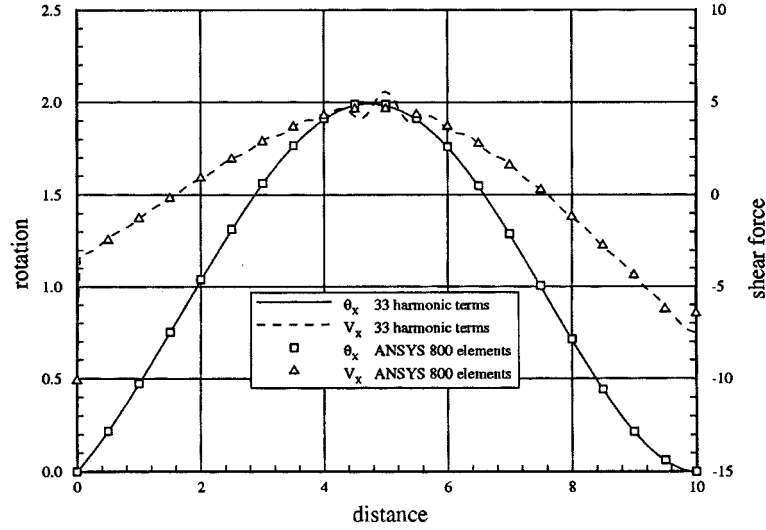
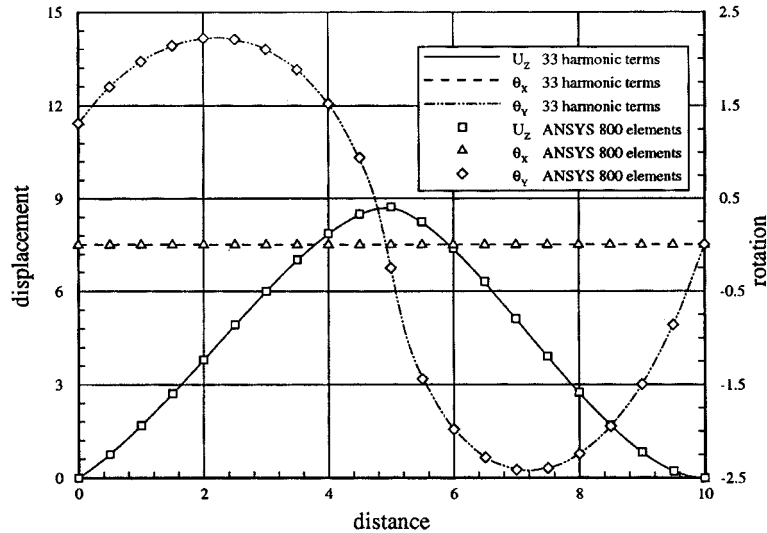
Fig. 10 Comparison of moment and shear force along $x=5$, plate IIFig. 11 Comparison of moment and shear force along $x=0$, plate II

Table 1 Comparison of computational performance

	Degrees of freedom	CPU time (sec)
ANSYS 800 elements	4680	46
ANSYS 3200 elements	18960	256
ANSYS 20000 elements	119400	10649
Fourier series 33 harmonic	528	62


 Fig. 12 Comparison of rotation and shear force along $y=0$, plate II

 Fig. 13 Comparison of displacement and rotation along $y=5$, plate II

$$\{d_s\}^H = \{bc_1^s \ bc_3^s \ bc_5^s \ bc_7^s\}^H, \quad \{d_p\}^H = [bc_1^p \ bc_3^p \ bc_5^p \ bc_7^p]^H$$

The above problem is analyzed herein by the approach with nine harmonics and ANSYS with 800 shell elements. Two results are compared. According to Fig. 6, the deformed shape is attributed to the thirty-three harmonics. In comparison of the two methods for displacement; rotation, normal force and bending moment of plate II are shown as Figs. 7-14. According to those figures, the results from both methods are nearly close to either displacements or forces on the interior plane or boundary line, except for the shear force along the connection boundary. This difference may be attributed to the twisting moments, as confirmed by a FEM mesh refinement. Herein, three cases of FEM mesh, i.e., 800, 3200, and 20000 elements, are selected to evaluate these

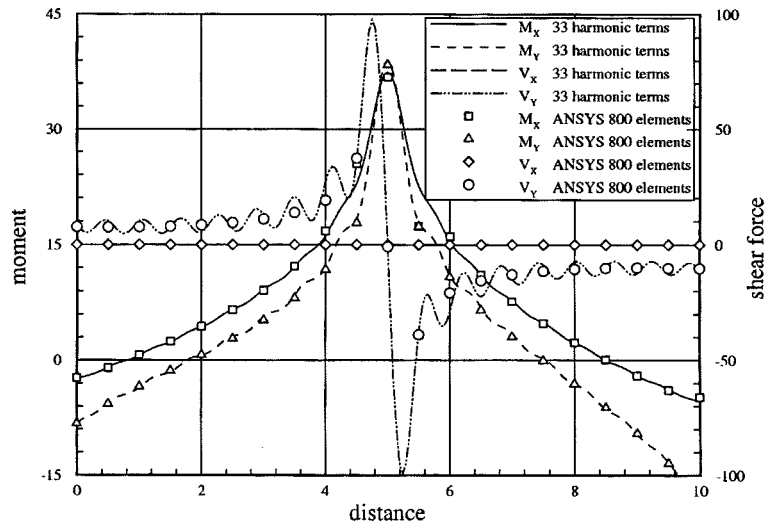


Fig. 14 Comparison of moment and shear force along $y=5$, plate II

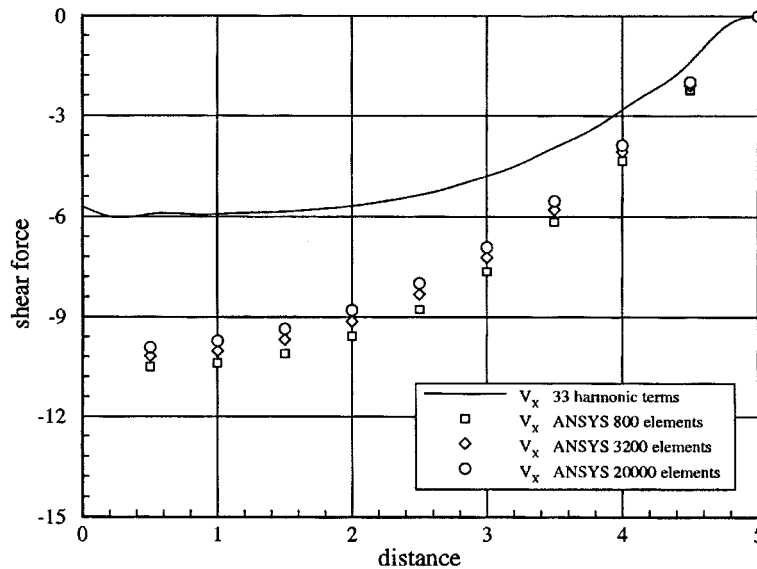


Fig. 15 Comparison of shear force along $y=0$, plate II

convergence characteristics. Fig. 15 compares the shear force results of both methods. Table 1 summarizes their computational performance. According to Fig. 15, FEM converges slowly in shear force computation. For the case of 20000 elements, 119400 degree of freedoms and 10649 sec CPU times have not converged to the same value as proposed method.

6. Conclusions

This work presents a simple and straightforward structural analysis method, and then applies it

to the static problem of plated structures, using the Fourier series expansion developed herein. Also the solution function of the governing equations with constant coefficients for in-plane and plate-bending problems is analytically derived. In addition, a non-co-planar connection of the plates is proposed for the structures with a complicated cross-section in a real spatial system. The efficient Fast Fourier Transform is also used to calculate discretely prescribed boundary conditions. It gives a lot of efficiency in the problem. In addition, lesser degrees of freedom are required than most available numerical methods. From the numerical example presented herein, we can conclude the following:

1. A much smaller amount of memory and a more minimal computational effort are required since no numerical integration is involved and lesser degrees of freedom are used.
2. Only the boundary of elements is required as a geometry description, thus indicating that the proposed approach can save a significant amount of time in problem-modeling.
3. Errors arise only along the boundary, since an approximation is made on the boundaries. In a domain's interior, the solution at each point can be obtained with a high degree of accuracy.
4. Owing to the "twisting moments", the shear force along the connection boundary of two plates is over-estimated and then converges slowly for FEM. This allows us to verify the effectiveness of the proposed method.

References

- ANSYS Version 5.1 User's Manual. (1994), Swanson Analysis Systems Inc. Houston, Pa.
- Boswell, L.F. and Zhang, S.H. (1983), "A box beam finite element for the elastic analysis of thin-walled Structures", *Thin-Walled Structures*, **1**(4), 353-383.
- Cheung, Y.K. (1976), *Finite Strip Method in Structural Analysis*, Pergammom Press, Elmsford, N.Y.
- Deng, J.C. and Cheng, F.P. (1997), "A Fourier series expansion method for two dimensional elastostatics", Submitted to *Computers & Structures*.
- Hartley, G.A. and Abdel-Akher, A. (1993), "Analysis of building frames", *Journal of Structural Engineering, ASCE*, **119**(2), 468-483.
- Hrabok, M.M. and Hrudley, T.M. (1983), "Finite element analysis in design of floor systems", *J. Struct. Div., ASCE*, **109**(4), 909-925.
- Irons, B.M. (1976), "The semiloof shell element", *Finite Elements for Thin Shells and Curved Members*, D.G. Ashwell and R.H. Gallagher, Eds., John Wiley and Sons, Inc., New York, N.Y. 197-222.
- Ishac, I.I. and Smith, T.R.G. (1985), "Approximations for moments in box girders", *Journal of the Structural Division, ASCE*, **116**(11), 2333-2341.
- Kang, L.C. (1992), "A Fourier series method for polygonal domains; large element computation for plates", Ph.D. thesis, Stanford University.
- Kristek, V. (1979), "Folded plate approach to analysis of shear wall systems and frame structures", *Proc., Institution of Civil Engineers*, Part 2, 1065-1075.
- Kukreti, A.R. and Rajapaksa, Y. (1990), "Analysis procedure for ribbed and gird plate systems used for bridge decks", *Journal of the Structural Division, ASCE*, **116**(2), 372-391.
- Maugh, L.C. and Pan, C.W. (1942), "Moments in continuous rectangular slabs on rigid supports", *Transactions, ASCE*, **107**, 1118-1142.
- Mikkola, M.J. and Paavola, J. (1980), "Finite element analysis of box girders", *Journal of the Structural Division, ASCE*, **106**(6), 1343-1357.
- Moffat, K.R. and Lim, P.T.K. (1977), "Some finite elements having particular application to box girder bridges", *Proceedings of the International Association of Bridges and Structural Engineering*, Zurich, Switzerland, Feb. 1-12.
- Moody, W.T. (1960), *Moments and Reactions for Rectangular Plates*. U.S. Department of Interior

Bureau of Reclamation Engineering Monograph.(27).

Ohga, M. Shigematsu, T. and Hara, T. (1991), "Boundary element transfer matrix method for plated structures", *Journal of Engineering Mechanics, ASCE*, **117**(11), 2509-2526.

Puckett, J.A. and Gutkowski, R.M. (1986), "Compound strip method for analysis of plate systems", *Journal of Structural Engineering, ASCE*, **112**(1), 121-138.

Timoshenko, S.P. and Woinowsky-Krieger, S. (1959). *Theory of Plates and Shells*, 2nd Ed., McGraw-Hill, New York, N.Y.

